

# Long-Term Environment Prediction for Model Predictive Control in Vehicles: Pattern Recognition upon Primitive Driving Behavior and Driver Condition

Karl-Falco Storm, Daniel Eckardt

Powertrain & Power Engineering  
IAV GmbH

Gifhorn, Germany

email: karl-falco.storm@alumni.tu-clausthal.de,  
daniel.eckardt@iav.de

Meng Zhang, Jörg Grieser,  
Michael Prilla, Andreas Rausch

Institute for Informatics  
Technische Universität Clausthal  
Goslar, Germany

email: {meng.zhang, joerg.grieser, michael.prilla,  
andreas.rausch}@tu-clausthal.de

**Abstract**—This paper evaluates the prediction accuracy of indeterministic environments. The exhaust aftertreatment for vehicles is used as a sample scenario, whose efficiency should be enhanced using pattern recognition techniques. It determines a control strategy to minimize exhaust emissions—whose volume, composition and temperature depends on the load and speed of the combustion engine. Since the engine being controlled by the accelerator pedal, the driving behavior needs to be predicted for adequate horizons. The new approach is simulated on the basis of driving data at different traffic scenarios, including urban, overland and motorway road types. The recorded driving behavior is examined location-based by transferring it into a dynamical number of primitive driving behavior classes. This way, traffic scenarios can be distinguished by using a relatively small set of data. Furthermore, the driving behavior does not have to be labeled, since information about it occurring is not required. In context with the task of vehicle control, possible changes in driving behavior due to a higher stress level have already been proven. Following this finding, driving behavior prediction is investigated in consideration of the driver’s condition. In the end, a benchmark is carried out to compare existing prediction methods of location-based pattern recognition. After presenting the findings, an outlook for possible future research is given.

*Keywords*-pattern recognition; long-term prediction; driver condition monitoring; primitive driving behavior; model predictive control.

## I. INTRODUCTION

From the perspective of control theory, ambient conditions are key input factors for a controller’s performance. In order to optimize the regulatory strategy of model predictive control systems regarding predefined targets, accurate predictions are needed. While this is very effective for deterministic and completed systems without randomness of future states, indeterministic processes and environments must be monitored closely. The environment is represented by signals of sensors observing it. Nevertheless, not all states and influences can be recognized, as the observation of certain values is impossible or technically too expensive.

Turning over towards driving behavior prediction, the actual state of the vehicle is observed by various on-board sensors. From this point of view, future conditions depend on possible car maneuvers performed by the driver. Besides driving

behavior classification, maneuver restricting driving environments are also an ongoing subject of research. These (partly indeterministic) restrictions include course of the road, speed limits, other traffic participants as well as weather and light conditions, for example. So, in order to generate accurate predictions, both factors—human and environmental—are considered. In this research, the predictions of indeterministic environments using pattern recognition techniques are evaluated and differentiated against existing approaches. This is done using driving behavior as a use case, including the driver’s condition for the first time.

### A. Motivation

In automotive field, slow control circuits like engine cooling, cabin climate conditioning gain efficiency from predictive control systems. The prediction of driving behavior is a key factor to many different applications in the automotive field. In this context, it is understood as the longitudinal and lateral control of a vehicle. Velocity and acceleration are mainly influenced via the accelerator pedal that affects the engine load [1]. To date, driving is mainly linked with human behavior, therefore, it is of an indeterministic nature. In conclusion, the effectivity depends on the driver’s pedal control, which represents his driving behavior as a function of the current traffic scenario.

The engine load and speed indirectly determine the amount and composition of the exhaust gas. Its general purpose is minimizing the emission of unwanted exhaust gas components. Each of its modules has got its own optimal operational temperature range, where each catalytic reaction performs best [1].

Looking at diesel engines in particular, an injection angle shift can lead to an increase in the exhaust gas and the exhaust aftertreatment system’s temperature. Compared to a cold system, a preheated exhaust aftertreatment system dramatically decreases the amount of NO<sub>x</sub> emitted at emission peaks due to better efficiency. But preheating also causes a slight increase in fuel consumption and, therefore, leads to additional CO<sub>2</sub> emission. While this strategy is usually pursued at the engine’s cold starting, it might also occur at normal operation [2]. For example, if the engine idles for a certain time (e.g., waiting at a road junction), the exhaust aftertreatment system cools down. Thereafter, at a possible acceleration, a huge amount of

exhaust gas may release the exhaust gas system untreated, until the light off temperature of the components are reached again. In this case, the exhaust aftertreatment gains efficiency, if preheating starts punctual. If it starts too early, fuel is wasted because of unnecessary heating. If it starts too late, the after-treatment efficiency still increases, but fuel consumption is higher than at optimal timing. The regeneration of the diesel particulate filter requires a constant high exhaust gas temperature. Ideal way, this process takes place at the time when a constant (higher) engine performance is present. This way, intensive preheating is not necessary again saving fuel and CO<sub>2</sub> emissions [1]-[4].

Both examples show that detailed knowledge of the upcoming engine load is significantly important for model predictive control. Therefore, improvements in prediction accuracy are investigated in this work.

### B. Content and Structure

This paper has the following structure: Section II gives an overview about predictive control systems, driving behavior, its prediction and driver condition detection. As a conclusion, a scientific gap is worked out in Section III. Thereafter, the new developed approach is described and explained with the aid of an example scenario in Section IV. Detailed structures and specifications of the algorithm are explained in the implementation part. In Section V, the experiment including test data generation is described. Finally, the findings are summarized and an outlook for possible future work is given in Section VI.

## II. RELATED WORK

Predictions of future ambient conditions can be done by using several approaches. A simple approach is the extrapolation of the actual observed status. Taking the vehicle condition as an example, constant speed, acceleration or accelerator pedal position (*KoGas*-model) are common techniques for short-term estimations in the matter of a few seconds, becoming more inexact for longer horizons [5][6]. But for the shown model predictive control systems, a horizon in the matter of minutes is required. Figure 1 shows a rough categorization of the related work. The different techniques are classified by their methodical approaches, their prediction horizons and their universality for being used at different road classes and traffic scenarios

Long-term predictions can be achieved by conflating navigation data (street type, road course, speed limit and ele-

vation profile) of the future route with the driver’s average (expected) driving behavior. Following this concept, functional models like *V85* are able to generate a velocity trajectory based on this navigation data. Further development of this concept was done by Müller et al. [7] and Ebersbach [8]. Both references describe functional models that learn the mean velocity deviation (compared to the speed limit) and acceleration behavior of an individual driver. Using this averaged driving behavior, good results are achieved for low traffic density at overland road. But these methods suffer at heavy traffic situation and at built-up areas, where the driving behavior is predominantly influenced by environmental factors like preceding vehicles [7]-[9]. Thus, concepts for taking the driving behavior of preceding vehicles into account have been developed, but they depend on environmental scanning, e.g., using an adaptive cruise control’s radar sensor [10].

Numerous authors addressed the prediction topic using machine learning techniques and statistical methods. They are also suitable to predict uncertainty by the distinction of traffic scenarios, e.g., using kernel density estimation [11] and Markov transition probabilities for discrete states [12]. Artificial Neural Networks (ANN) proved to be an accurate way of predicting driving behavior under uncertain conditions [6]. Nevertheless, ANN’s high demand of labeled learning data is a downside.

Clustering algorithms are commonly used to distinguish traffic scenarios, thus potentially receiving better results [13]-[15]. Features can be abstracted from the raw signals, their histograms or distributions. Both pattern recognition techniques have almost exclusively been used on single traffic scenarios yet, but they do offer promising possibilities for universal approaches even with small sets of data [10].

So far, driving behavior prediction has commonly been described from a data’s point of view. But in this context, the human machine interaction’s point of view is another important field of investigation, because each driver has got his individual behavior in different driving situations. Besides physical and legal restrictions, the personal preferences of the driver may depend on a wide field of different factors, giving it indeterministic characteristics [8]. They can be classified into stable (1) and variable (2) factors, depending on the person (a) or a certain situation (b), e.g., sociodemographic characteristics (1a), driving ability (2a), traffic environment (2a) and weather (2b) [14][16]. By observing the mental and emotional state of the driver, some conclusions might be drawn— e.g., a negligent driving behavior while being pressed for time.

Mental workload estimation of humans has been investigated for an even longer period. In general, five different techniques of state evaluation are derived from literature (Figure 2). They include direct measurement and iterative physiologic measurements, self-assessment, observing via attention tests to make assumption from ambient conditions (*Digital Emotions*). All methods can deliver exact results, only if appropriate analysis models are used and calibrated before.

A fusion of different physiological measurements gives good results if the physical impact of the environment can be controlled (e.g., movements, temperature fluctuations). Attention tests and repetitive surveys are not very suitable for continuous measuring, because they affect the actual state of the

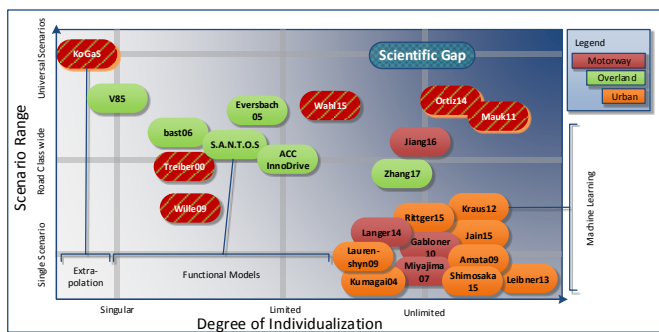


Figure 1. Categorization of driver stress detection methods.

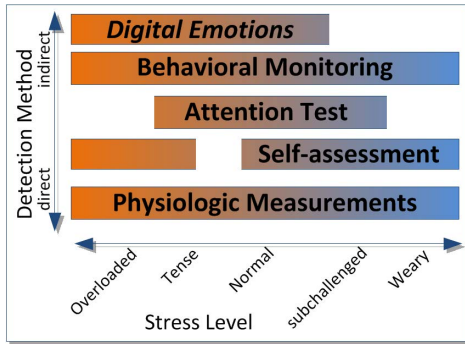


Figure 2. Categorization of driver stress detection methods.

experimentee by giving him an additional task. For self-assessment, slight stress may not be detected by the experimentee. Behavior observing can be done by rating actions, movements and posture. This usually requires a qualified investigator or expertise. Finally, *Digital Emotion* summarizes techniques for making assumptions of the experimentee by observing ambient conditions. For driving tasks, this includes the interpretation of external factors that might affect the driver condition such as intense traffic or aggressive behavior. Of course, a fusion of all five methods delivers highly precise information [17].

While matching workload onto sensor data is relatively easy, this does not count other way around—detecting stress from sensor data. According to the valence-arousal model, stress is a combination of mental workload and negative emotions. A great variety of physiological signals are capable of drawing conclusions about the mental load and the emotional state after setting up a suitable stress model [15][18].

Pulse data and the Galvanic Skin Response (GSR) are easy to measure and frequently used in activity trackers. While studies proofed their reliability for scientific applications, open low-cost platforms for scientific research are yet hard to find. This also applies for the evaluation methods apart from classical methods. In terms of data analysis, features are extracted and interpreted from the respective raw sensor signals. The Heart Rate Variability (HRV) is derived from time difference between two subsequent heart beats, which can be used as a stress measurand. High mental workload and emotional stress usually cause the HRV to decrease. Photoplethysmo Graphic Sensors (PPG) allow the measurement of pulse data by simply recording the capacity of reflection at suitable skin areas. Because this signal is not identical to electrocardiograms, the derivation of HRV is inexact [19][20].

GSR analysis is another approach that is issued frequently. An internal or external stimulus leads to a sudden decrease with slow recovery of skin resistance because of sweat gland activity within seconds. Therefore, the palm of the hand and sole are suited best for measuring. The number and intensity of peaks is determined by a deconvolution analysis [21]. Emotional states are usually detected using non-heuristic methods [22], necessitating a valid emotional model to be established in advance. Relying on physiological measurements alone, sensor accuracy and interpretation accuracy together tend to be around 45-65% [21][23].

In context with the task of vehicle control, possible changes in driving behavior due to a higher stress level have already been proven [16]. Vice versa, stress and traffic scenarios have been related by Heinrich [17] and Yamaguchi et al. [24]. Based on their findings, the prediction of future driver workload is possible after a sufficient training period. But studies also showed that the manner and effects are individual, as the experimentee's driving behavior responds different in complex and stressful situations. Therefore, no general valid conclusions can be drawn [25].

### III. SCIENTIFIC GAP AND RESEARCH QUESTION

Machine learning techniques for predicting the future environment have already been described in numerous publications, proving their effectivity in certain traffic scenarios. But they have not yet been investigated for a universal usage. Concerning driving behavior, long term predictions are currently generated based on functional models and navigation data.

For an extensive traffic scenario distinction, these models need a wider range of input data about road conditions, weather, the driver's intention as well as other traffic participants. It is not possible yet to gather all the necessary information via sensors, even if cloud services and Car2X technologies extend their *perception range*. High definition map data are an additional cost factor not to be scored, as it needs to be updated frequently. Especially for cars with simple specification, this kind of information is not available yet, leaving traffic guidance-based predictions at an insufficient data situation. Furthermore, a priori distinction of traffic scenarios is needed for functional models, equivalent to labels for training artificial neural networks.

Keeping this in mind, a pattern recognition technique should be developed that relies on simple and limited data input, offering a wider variety of traffic scenarios to be distinguished. Also, location-based predictions allow considering local particularities if a driver travels repeatedly on the same route, learning from the driver individual behavior. The observation of the driver's conditions regarding his emotion and stress level should be evaluated in order to enhance the prediction effectiveness.

### IV. PATTERN RECOGNITION

For image recognition, patterns are typical detected and assigned based on the training of an artificial neural network with a pre-labeled dataset. For signal paths, labeling can be done analog, describing certain ambient scenarios that need to be defined in advance. Conversely, pattern recognition focuses on similar recurring patterns of an observed value. This implies that certain patterns occur regularly in any similar form and order. Clustering algorithms allow the detection and specification of similar patterns by the comparison of the input data, opening up for a wider set of dynamical defined scenarios (classes). Therefore, the signals need to be split into discrete sections on which clustering is applied. In order to combine the individual patterns for long-term predictions, they need to be connected in any particular order. This can be achieved using transition matrices that keep track of the signals during pattern classification. Afterwards, transition possibilities are derived from that.

For a model-based exhaust aftertreatment control system, the timeline of the engine load and speed are of special interest for estimating the future exhaust volume flow. It is mainly influenced by the driver’s usage of the accelerator pedal; for first approximation his input needs to be predicted. Generally, the resolution of the engine load can be reduced into several discrete classes, depending on the respective application.

At this point, longitudinal acceleration is graded into primitive driving behavior classified by the following (see Figure 3, deep-red graph): high (1-2) or medium (3) engine load for an increase of velocity or start-up, lower (4) engine load for constant velocity and idle (5-6) for deceleration and coasting. The velocity is classified in relation to the actual speed limit (or a location-based mean speed, if map data are unavailable) to approximate certain primitive traffic scenarios. The classes include halt or stop and go (0), traffic jam (1), minor slow-down (2), normal velocity (2-3) and faster velocity scenarios (3-4). Furthermore, the driving behavior does not need to be linked to factors causing it [10].

Conclusions are rather drawn by evaluating the location-based likelihood of their occurrence and thus, can be inter-linked iteratively for long-term predictions. Driving behavior and prediction knowledge are saved inside map database for it to be used location depended. Figure 3 shows how sample data of a route section is translated into its corresponding primitive driving behavior pattern using the introduced heuristic rules.

For the generation of a knowledge base, all previous observed and recorded trips are separated among identical sections borders to keep them comparable. Useful sectioning can be done by the means of road type transitions and intersections (again, if no map data are available, sectioning should be derived from a batch of recorded data on the same route). Figure 4 shows four sample classes of driving behavior that have been identified via clustering, comparing the similarity between each other. Each class represents the driving through a corresponding traffic scenario on the same route section, e.g., rather clear road (left and mid-left) or an intense traffic scenario (far right). This way, changing traffic conditions between each section are considered just by their impact on the driving behavior.

Table I shows how a route is separated into section (s1-s8) by its map-data properties listed in the second column. In fact, all sections are designed to overlap each other enhancing their functionality close to their fringes. Inside each section, a number of discrete classes (N) describe the observed driving behavior pattern. The number of classes is determined dynamically upon the similarity of the recorded trips; it varies between one and a useful upper limit. For example, on a motorway, only three to four different patterns are distinguished,

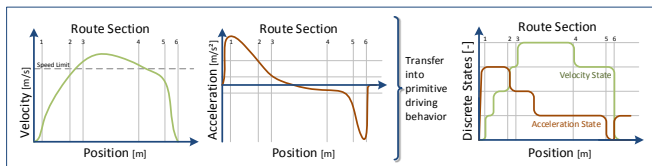


Figure 3. Deriving primitive driving behavior patterns from velocity and acceleration signals; a start-to-stop example.

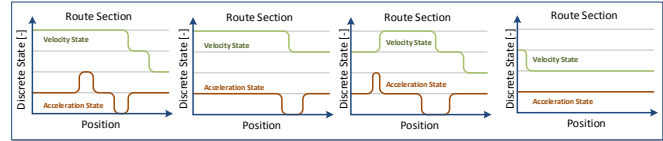


Figure 4. Four discrete traffic scenarios (classes) represented by their corresponding primitive driving behavior patterns.

whereas in urban areas many different patterns may.

Inside each class, the driving behavior (velocity and acceleration) is averaged over all assigned measuring runs. The right side of Table I shows 23 laps being assigned to eight clusters inside section s2. For each pattern-class (and their both section transition), a transition matrix keeps track of the classification flow for each single measuring run (far right). This allows building up statistical transition relationships between the section’s classes. Referring to Markov property, the allocation probabilities for subsequent sections only depend on the actual class rather than on the previous classes (see Figure 5). As soon as the knowledge is built for all necessary route sections, prediction is possible. Using the elements with the highest rating, class across predictions becomes possible. Then, when the first couple of meters are passed on the first section (s1), the actual observed driving behavior is matched to its best fitting classes inside the knowledge base. Thus, the algorithm chooses the most appropriate class for predicting. Because of changing transition probabilities, a change of the matched driving behavior class also leads to changes for the interlinked classes of the following route sections.

Regarding the driver, observations of his conditions are also reduced into primitive patterns. They are combined from the self-assessment inside the valence-arousal state space and the physiological monitoring. Figure 6 shows combined ratings matched to the course of the route. Certain positions show a peak due to brief events (red traffic lights, hard braking etc.). As a result, pattern recognition methods need to process multi-dimensional input data. Otherwise, a combination of the evaluations needs to be calculated (e.g., by multiplication).

## V. SIMULATION AND EVALUATION

A simulation was set up to evaluate the pattern recognition methods shown in Figure 8, with and without the driver’s condition consideration, compared to reference methods. In order to make it statistically sound, the overall sample size must reach a relatively high quantity which makes real-time in-car testing impossible. Therefore, a set of training data was recorded to simulate the prediction methods at different traffic environments and scenarios inside a virtual simulation environment. After short explorative research including a basic validation of the approach, the necessary sample size was estimated. Because the size exceeds the number of possible real-time experiments, a MATLAB toolbox was set up for a simulative evaluation. Hereafter, the measuring runs, the data recording and their preparation is described. Afterwards, the implemented methods are outlined, and prediction results are presented.



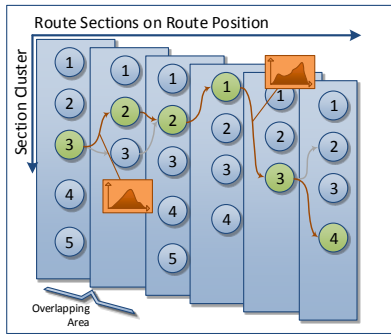


Figure 5. Interlinked driving style classes allow long-term prediction horizons using Markov property.

A. Data Preparation

In order to simulate the reduction of driving behavior, a large pool of real driving data needs to be recorded in advance. This was achieved by utilizing an experimentee that drove repetitive on a predefined test route. The runs were recorded using a position tracker, a physiological recorder and an event logger. Over 60 completed laps of mixed urban, overland and motorway driving environment—a total of 3,400 km—has been recorded, including 31 laps with GSR and Pulse monitoring of the driver. A Volkswagen Golf Mk4 was used as test vehicle. It is equipped with a manual gear shift and a retrofitted cruise control which was used as reference driving behavior.

Physiological data has been recorded using a *Shimmer GSR+* sensor recorder equipped with two GSR electrodes and a PPG fingertip sensor. Figure 7 shows the setup for the measuring runs: The sensor recorder was attached to the left arm to minimize interruption due to finger movements during steering and gear changes (middle). With the help of an event logger software set up, inputs like self-assessment and possible external stimuli are logged (far right). The latter includes temporal stimuli, precipitation, lighting and temperature conditions to contextualize the self-reported emotions.

All measuring data was later mapped on *HERE WeGo* navigation data and interpolated 1 m resolution. Velocity and acceleration data has been adjusted for plausibility considering the vehicle’s performance. HRV and skin conductivity features were extracted from the physiological sensor data using the *MATLAB* Toolboxes *Ledalab* (GSR) and *Pan-Tomp-*

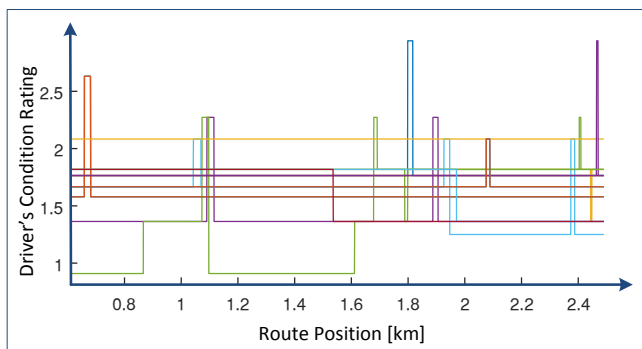


Figure 6. Comparison of several driver’s conditioning ratings in relation of the route position. Peaks marking special events of arousal.



Figure 7. Experimentee with GSR electrodes and PGG fingertip sensor (left and middle); Event logger interface (right).

kins (HR) with *KubiosHVR* Standard. They were combined with the driver’s self-reports keeping track of the mood and workload. An ordinal evaluation table is utilized for converting the single inputs into an ordinal stress rating (Figure 6).

B. Implementation of the prediction methods

For the final benchmark, five prediction methods were implemented as shown in Figure 8. Two of them were used as a reference: The **Speed Limits** (SL, 1) for the route were retrieved via *HERE WeGo* in advanced. Speed limit transitions were smoothed out using the test vehicle’s lateral acceleration capabilities. This way, a rather naïve prediction was generated, representing a minimum solution. Figure 9 shows the speed limit (black line) for a latter part of the test route.

An **Adaptive Functional Model** (AFM, 2) was implemented using *MATLAB Simulink*. It is capable of generating predictions-based on velocity deviation (as a function of the speed limit) and observed acceleration behavior (as a function of the vehicle speed). Every single run is trained in advanced to ensure this method to deliver the best possible outcome. Even though this kind of training would not be possible in real-time evaluation, training the AFM using other recorded laps give detrimental results. Figure 9 shows the speed profiles generated with this model. For better performance at traffic lights and intersection (pink, area of interest), an additional feature was integrated into the functional model to give it further advantages over straight trajectories. Taking all recorded test laps as a basis, statistical information about the chance of stopping were evaluated. If halt probability was over 50 % inside the according region of interest, the average velocity passing it, is added to the trajectory.

Next up, two different clustering methods are described: **Hierarchical Clustering** (HC, 3) and **Growing Neural Gas** using driving behavior (GNG, 4) and additional Driver Condi-

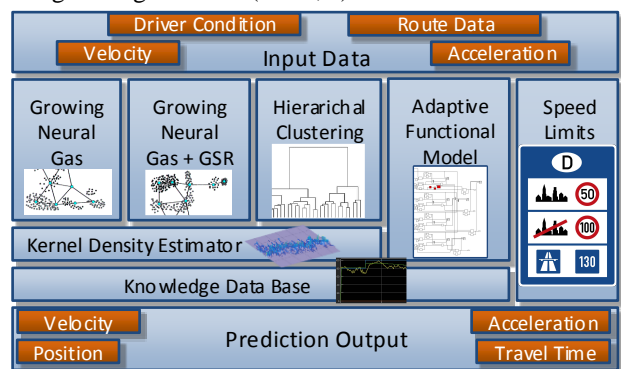


Figure 8. Overview of prediction methods used for the Benchmark.

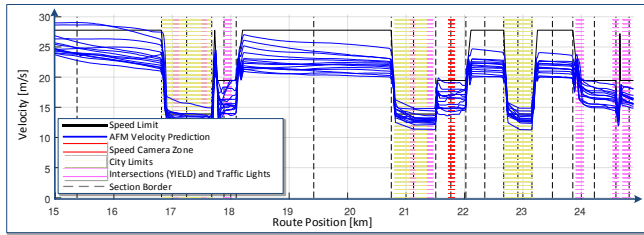


Figure 9. Generation of 14 velocity prediction trajectories using the adaptive functional model (AFM) reference.

tions (DC, 5) as training data. Hierarchical clustering using Ward’s Method is based on the Euclidian distance between each set of features. In this case, the distances are calculated between the primitive velocity and acceleration pattern (see Figure 4). The distances between primitive driving patterns can be visualized using linkage tree. In Figure 10, the corresponding Euclidean distance values of 23 driving profiles mark the border between aggregated and independent clustering classes. The optimal number of classes is determined by minimizing the inter-cluster distances (that is, minimizing the sum of class internal distance values), depicted by the orange bar for  $L^2 = 500$ . In a last step, all driving profiles that remained linked are merged into a single class.

In order to get predicted behavior for every class, velocity and acceleration data are averaged using a kernel density estimator. Then, the primitive driving behavior is derived from it. A Growing neural gas implementation is used with two distinct data sets. Unlike hierarchical clustering, it allows multi-dimensional feature sets; A priori combination is not necessary. Also, the dynamical optimization of the class numbers is already integrated [26].

For deciding which class (prediction) to choose, the same distance metrics from HC are used for comparing the actual driving behavior with the knowledge base. At the end of each section, the subsequent classes are determined considering transition probabilities. Figure 11 shows the prediction of a measuring run (solid green line) being iteratively calculated every 10 m (dotted blue line) on the left-hand side. At the 11.5 km mark, the road type changes from two-lane motorway to a single-lane overland road. A change in prediction accuracy is directly visible due to an increased variance. The speed limit (black) is drawn as reference.

C. Simulation Runs

First of all, the recorded laps were separated randomly using a lottery, resulting in 75 % (23) training data and 25 % (8)

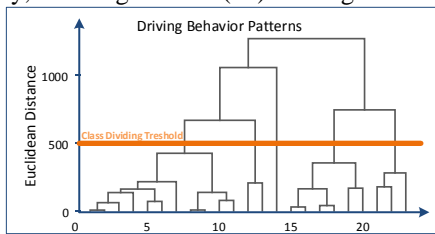


Figure 10. Dendrogram of 23 driving profiles being divided into five classes according to their similarity.

test data sets. After separation, knowledge databases were generated for all clustering methods using parallel processing. For benchmarking the methods at different traffic environments, four test areas were defined for all three road types: urban, overland and motorway. Inside each area, the actual start of prediction is then determined randomly for each simulation iteration. The prediction horizon is set to 90 seconds with 150 m being the minimum distance. This way, the horizon usually reaches from 1250 to 2500 m, depending on the actual vehicle speed at the prediction start. All methods then use the same end horizon to keep them comparable. With eight simulation runs in total, the number of simulated predictions reveals to 768 iterations (8 iterations × 8 tested profiles × 12 evaluation areas).

For each iteration, the virtual Volkswagen drives up to the next prediction start point. After arriving, all prediction methods calculate velocity and acceleration trajectories within prediction horizon. Figure 11 shows two sample predictions generated by AFM (dotted grey) and HC (dotted blue) on the right-hand side. The point where the prediction starts is indicated by a blue circle, located at the original trajectory (solid green). On the left side, a main road example is shown. AFM prediction is visibly better for the first 700 meters as it is closer to the original trajectory. Looking at the acceleration, HC gets it quite well for position 13.1 to 13.5 km where both trajectories decrease. On the right side, a mixed urban (yellow) and ex-urban scenario are shown. Obviously, a stop-and-go traffic scenario can be identified at distance 22.5 to 24 km when velocity drops below 5 m/s. This time, the pattern recognition method clearly outruns the functional model as it predicts velocity and acceleration behavior quite well. Nevertheless, prediction here is shown on a location-based which is preferable for visual evaluation. Physically correct is a time-based prediction which is harder to depict.

D. Simulation Results

After generating all predictions, the respective trajectories are compared to the real driving behavior. For both signals, velocity and acceleration, the Root-Mean-Square Error (RMSE) is calculated according to their time-dependent signal paths (Table II). The best performing values are highlighted. For the driving time, the absolute difference at the end of the prediction horizon is used. After completing twelve iterative runs, the simulation starts over using the subsequent lap. Negligible difference between several simulations proved the sample size of 768 to be statistically sound for this simulation (in fact, within a 95 % confidence interval).

In order to apply statistical analysis, a distribution function has been fitted to the RMSE values and the absolute driving time deviation. It turned out that a log-normal distribution fits them perfectly, allowing a symmetrical boxplot representation of the results. Figure 12 shows the aggregated results of the simulation runs. The boxplots illustrate the logarithmized RMSE distribution of acceleration, velocity and time prediction. The diamond represents the median of all measured values. Outliers are represented by spots outside the whiskers

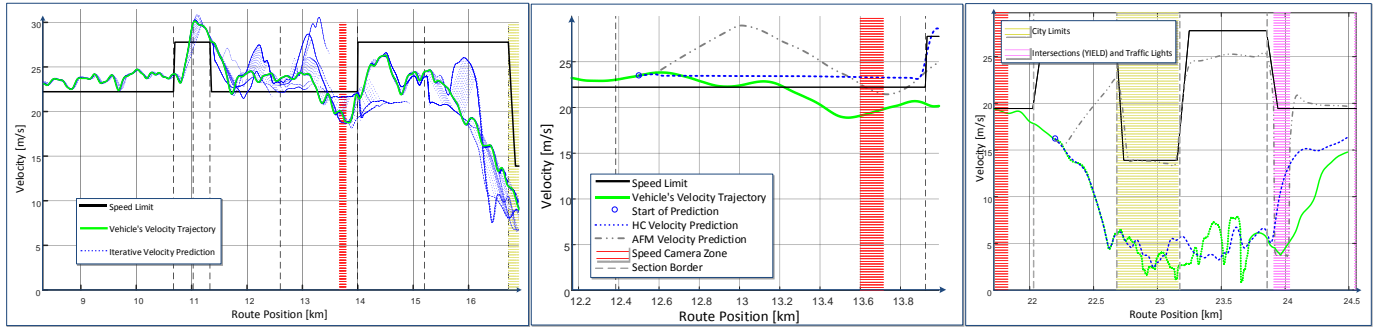


Figure 11. Iterative velocity prediction every 10 m (blue, dotted) using HC and a prediction horizon of 30 s (left figure). Two samples of a single velocity prediction comparing HC and AFM including local features (right figures).

The upper plots show direct comparison between the reference methods (SL, AFM) and the three pattern recognition methods (HC, GNG, DC). All three disciplines are dominated by the pattern recognition methods—they have lower logarithmized RMSE values, and thus, lower mean errors (see Table 2). At urban, ex-urban and motorway scenarios, the mean acceleration difference is 0.076 m/s<sup>2</sup> using the naïve speed limit-based prediction. The adaptive functional model-based prediction only improves little by 5 % (0.072 m/s<sup>2</sup>). Pattern recognition greatly improves the accuracy by 37.5 % (0.045 m/s<sup>2</sup>) using Growing neural gas. Velocity and driving time predictions show a similar picture. While pattern recognition improves velocity prediction by 35 % (0.77 vs. 0.50 m/s for AFM vs HC), driving time, which is the sum of all velocity deviations at the end of the prediction horizon, pattern recognition methods reduce the mean error by 30 % from 8.6 s to 6.1 s.

The lower boxplots show the detailed results for each road type. As pattern recognition dominates, both references methods (HC and SL) are left out now to obtain a better overview.

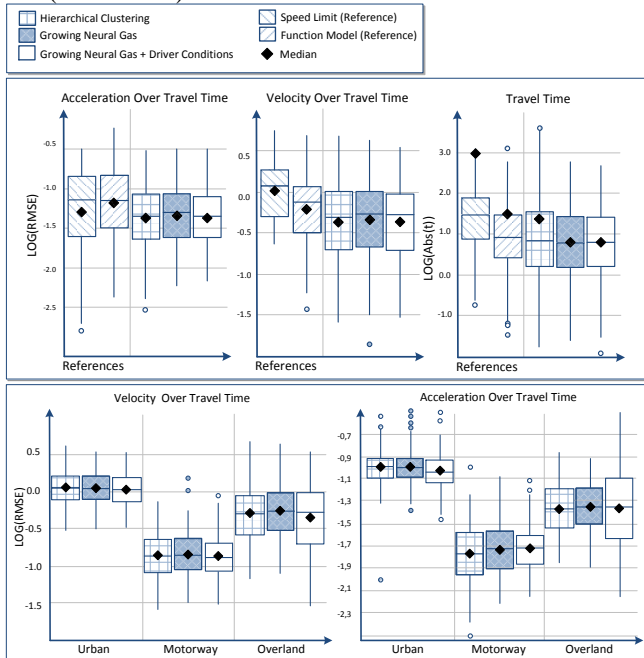


Figure 12. Detailed boxplots of the simulation results (n: 768, 90 s horizon).

On the left third, the logarithmized RMSE for velocity prediction are shown, arranged in urban, overland and motorway traffic environments. On the right, acceleration prediction is shown in the same order. Overall, predictions for motorway scenario got the highest accuracy, being more than 7.5 times better than urban and more than 3.5 times better than at overland scenarios; Five times or 2.5 times for acceleration, respectively. It is worth mentioning that Growing neural gas using driver condition patterns performs best at built-up areas. Velocity predictions are 3 % better, whereas the acceleration performance increases about 8 %. The mean driving time deviation is 0.02 s better, which is an improvement of 2 %. All other scenarios are not dominated by DC.

In terms of computing time, the SL reference uses almost no resources being plausibilized only. Next up, as AFM only learns the actual run, computational time is negligible. The situation for clustering algorithms is quite different. Knowledge base generation using Growing neural gas algorithm uses up a lot of resources and calculation time doubled with every additional driving profile. Hierarchical clustering performed most effectively by comparison.

## VI. CONCLUSION AND FUTURE WORK

In this work, it has been shown that location-based pattern recognition is capable of delivering long term driving behavior predictions. It also shows a significant higher accuracy compared to traditional functional models. Also, the consideration of the driver condition does have advantages at traffic scenarios with great external influences, improving predictions by another 3 to 8 % (Figure 12, lower part).

At this point, it is rather unclear whether the driver’s condition really influenced the driving behavior at urban scenarios, or if external factors like traffic intensity influenced the drivers’ conditions. In the latter case, ambient conditions may become “visible” for the pattern recognition method. For other traffic environments, benefit from computationally expensive Growing neural gas over Hierarchical clustering algorithm was no issue.

For further validation of the concept, the following changes in the experimental designs are recommended: Using a better motorized test vehicle and recording its CAN-Bus data directly. The set-up of a stress model using valence-arousal model, a stimuli session should be completed in advanced, in order to perform a qualitative analysis upon the driver’s condition [25]. Five to ten different experimentees

should participate in the test run in order to evaluate the prediction performance according their individual driving behavior. Looking at driving behavior in particular, the respective traffic scenarios should be captured and analyzed detailed.

On the algorithm's side, prediction methods based on artificial neural networks should be included into the benchmark as well. Furthermore, the necessary level of detail for model predictive control should be considered in the evaluation. Therefore, the simulation of real physical processes and the effect of variable prediction horizons length may be considered as well.

## REFERENCES

- [1] S. Pischinger and U. Seiffert, "Handbuch Kraftfahrzeugtechnik," (Automotive Engineering), Springer Vieweg, 2016.
- [2] R. Plöntzke, S. Naumov, M.-C. Bartsch, A. Lechmann, and C. Stebner, "Nutzung prädiktiver Streckendaten zur Minimierung von Verbrauch und Emissionen in allen Fahrsituationen," (Minimizing Consumption and Emissions Using Predictive Route Data), Desden: FAD, 2017.
- [3] K. R. Neuhäuser, "Entwicklung einer Temperaturregelung und Vorsteuerung für die Dieselpartikelfilter-Regeneration mit experimenteller Bedatung," (Development of a Temperature Control and Pilot Control for the Regeneration of DPF), Berlin, 2016.
- [4] T. Grahle, M. Tonne, A. Wiedersberg, and T. Zsebedits, "Regeneration des Partikelfilters mithilfe von Navigationsdaten," (DPF Regeneration with the Help of Route Data), Motorische Zeitschrift, vol. 77, no. 1, 2016, pp. 16-22.
- [5] D. Heinrich, "Modelling the driver's behavior to investigate the dynamic loads in the drivetrain," Forschungsberichte IPEK, vol. 92, 2016.
- [6] S. Lefèvre, C. Sun, R. Bajcsy, and C. Laugier, "Comparison of parametric and non-parametric approaches for vehicle speed prediction," American Control Conference, 2014.
- [7] M. Müller, M. Reif, M. Pandit, Staiger, and Wolfgang, "A predictive gear shift system for motor vehicles using environmental data," Automatisierungstechnik, vol. 52, no. 4, 2004, pp. 180-188.
- [8] D. Ebersbach, "Entwurfstechnische Grundlagen für ein Fahrerassistenzsystem zur Unterstützung des Fahrers bei der Wahl seiner Geschwindigkeit," (Speed Selection ADAS), Dresden, 2004.
- [9] H.-G. Wahl, "Optimale Regelung eines Prädiktiven Energiemanagements von Hybridfahrzeugen," (Optimal Model Predictive Control for Hybrid Vehicles), Karlsruhe, 2015.
- [10] M. Zhang, K.-F. Storm, and A. Rausch, "Recognition and forecast of driving behavior-based on self-learning algorithms," in Hybrid and Electric Vehicles, Braunschweig, 2017, pp. 216.
- [11] T. Kumagai and M. Akamatsu, "Modelling and prediction of driving behavior," in 2nd International Symposium on Measurement, Analysis and Modeling of Human Functions / 1st Mediterranean Conference on Measurement, Genova, 2004.
- [12] T. Mauk, "Selbstlernende, zuverlässigkeitsorientierte Prädiktion energetisch relevanter Größen im Kraftfahrzeug," (Selflearning, Reliability-Criented Prediction of Energetic Relevant Dimensions), Stuttgart, 2011.
- [13] A. Laurensbyn, L. Åström, and K. Brundell-Freij, "From speed profile data to analysis of behaviour—Classification by Pattern Recognition Techniques," IATSS RESEARCH, vol. 33, no. 2, 2009, pp. 88-89.
- [14] M. Liebner, F. Klanner, M. Baumann, C. Ruhhammer, and C. Stiller, "Velocity-based driver intent inference at urban intersections in the presence of preceding vehicles," IEEE Intelligent Transportation Systems Magazine, vol. 5, no. 2, 2013, pp. 10-21.
- [15] Z. F. Quek and E. Ng, "Driver identification by driving style," Stanford, 2013.
- [16] H. Holte, "Einflussfaktoren auf das Fahrverhalten und das Unfallrisiko junger Fahrerinnen und Fahrer," (Treats on Driving Behavior and Crash Risks of Young Drivers), in Berichte der Bundesanstalt für Straßenwesen, no. M 229, 2012.
- [17] F. Heinrich, "Vorhersage der Fahrerbelastung während der Fahrt," (Prediction of the Driver's Stress Level During Driving), Stuttgart, 2012.
- [18] M. B. H. Wiem, and Z. Lachiri, "Emotion classification in arousal valence model using MAHNOB-HCI database," in International Journal of Advanced Computer Science and Applications, vol. 8, no. 03, 2017, pp. 318-323.
- [19] P. Rainville, A. Becharab, N. Naqvib, and A. R. Damasioc, "Basic emotions are associated with distinct patterns of cardiorespiratory activity," in International Journal of Psychophysiology, vol. 61, 2006, pp. 5-18.
- [20] M. Rollin, M. Atkinson, and W. A. Tiller, "The effects of emotions on short-term power spectrum analysis of heart rate variability," in The American Journal of Cardiology, vol. 76, no. 14, 1995, pp. 1089-1093.
- [21] Y. Shi, M. H. Nguyen, P. Blitz, B. French, and S. Fisk, "Personalized stress detection from physiological measurements," Pittsburgh, 2010.
- [22] R. E. W. Jenke, "Static and dynamic methods for emotion recognition from physiological signals," München, 2015.
- [23] C. McCarthy, N. Pradhan, C. Redpath, and A. Adler, "Validation of the Empatica E4 wristband," in Student Conference (ISC), 2016 IEEE EMBS International, Ottawa, IEEE, 2016, pp. 1-4.
- [24] M. Yamaguchi, J. Wakasugi, and J. Sakakima, "Evaluation of driver stress using biomarker in motor-vehicle driving simulator," in EMBS Annual International Conference, New York City, IEEE, 2006.
- [25] M. Soleymani and J. Lichtenauer, "A multimodal database for affect recognition and implicit tagging," in Transactions of Affective Computing, vol. 3, no. 1, 2012.
- [26] S. M. K. Heris, "Neural gas and GNG networks," in MATLAB, 2015-08-28. <http://yarpiz.com/77/ypml111-neural-gas-network> [Accessed 2018-02-02].
- [27] P. J. Lang, M. K. Greenwald, M. M. Bradley, and A. O. Hamm, "Looking at pictures: affective, facial, visceral, and behavioral reactions," in Psychophysiology, no. 30, 1993, pp. 261-273.
- [28] M. Singh and A. Bin Queyam, "Stress detection in automobile drivers using physiological parameters: a review," in IJEE, vol. 5, no. 2, 2013, pp. 1-5.
- [29] J. E. Meseguer, C. T. Calafate, and J. C. Cano, "Driving styles: assessing the correlation of driving behavior with heart rate changes," València, 2017.



TABLE I. DIVIDING A ROUTE INTO DISCRETE SECTIONS, SAMPLE CLUSTERING OF 23 MEASURING RUNS.

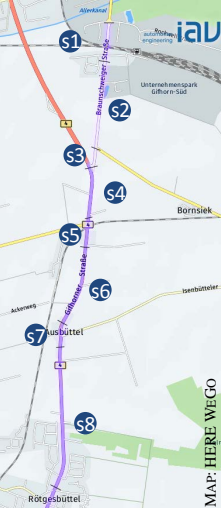
Map Visualisation of the Route	Map Data	Section Type	Number of Classes per Section	Number of Trips per Class	Transitions' Probability											
	Road Type Speed Limit Intersections Traffic Lights [...]	s1: Urban	N = 9 Classes	<table border="1"> <tr><td>Cluster 1: 3</td></tr> <tr><td>Cluster 2: 2</td></tr> <tr><td>Cluster 3: 3</td></tr> <tr><td>Cluster 4: <b>6</b></td></tr> <tr><td>Cluster 5: 1</td></tr> <tr><td>Cluster 6: 2</td></tr> <tr><td>Cluster 7: 4</td></tr> <tr><td>Cluster 8: 2</td></tr> <tr><td><math>\Sigma</math> 23 Trips</td></tr> </table>	Cluster 1: 3	Cluster 2: 2	Cluster 3: 3	Cluster 4: <b>6</b>	Cluster 5: 1	Cluster 6: 2	Cluster 7: 4	Cluster 8: 2	$\Sigma$ 23 Trips	<table border="1"> <tr> <td>Previous Section (s1) From Cluster 3: <b>6</b>/16</td> </tr> <tr> <td>Subsequent Section (s3) To Cluster 4: 1/<b>6</b> To Cluster 8: 4/<b>6</b> To Cluster 9: 1/<b>6</b></td> </tr> </table>	Previous Section (s1) From Cluster 3: <b>6</b> /16	Subsequent Section (s3) To Cluster 4: 1/ <b>6</b> To Cluster 8: 4/ <b>6</b> To Cluster 9: 1/ <b>6</b>
		Cluster 1: 3														
		Cluster 2: 2														
		Cluster 3: 3														
		Cluster 4: <b>6</b>														
		Cluster 5: 1														
		Cluster 6: 2														
		Cluster 7: 4														
Cluster 8: 2																
$\Sigma$ 23 Trips																
Previous Section (s1) From Cluster 3: <b>6</b> /16																
Subsequent Section (s3) To Cluster 4: 1/ <b>6</b> To Cluster 8: 4/ <b>6</b> To Cluster 9: 1/ <b>6</b>																
s2: Overland	N = 8 Classes															
s3: Overland	N = 4 Classes															
s4: Overland	N = 6 Classes															
s5: Urban	N = 9 Classes															
s6: Overland	N = 6 Classes															
s7: Urban	N = 6 Classes															
s8: Overland	N = 7 Classes															
[...]	[...]	[...]	[...]													

TABLE II. MEAN RMSE AND COMPUTING TIME FOR ALL SIMULATED PREDICTION METHODS.

	SL			AFM			HC			GNG			DC		
	$\frac{m}{s}$	$\frac{m}{s^2}$	s	$\frac{m}{s}$	$\frac{m}{s^2}$	s	$\frac{m}{s}$	$\frac{m}{s^2}$	s	$\frac{m}{s}$	$\frac{m}{s^2}$	s	$\frac{m}{s}$	$\frac{m}{s^2}$	s
Urban	2.04	0.157	80.9	1.346	1.193	<b>24.7</b>	1.099	0.102	39.9	1.109	0.101	33.7	<b>1.077</b>	<b>0.092</b>	34.4
Motorway	0.43	<b>0.013</b>	7.75	0.21	0.021	2.09	<b>0.137</b>	0.019	1.25	0.143	0.019	<b>1.21</b>	<b>0.137</b>	0.020	1.28
Overland	0.90	0.060	15.6	0.80	0.070	10.5	<b>0.515</b>	0.043	7.11	0.543	0.045	7.80	0.533	<b>0.040</b>	<b>6.70</b>
Combined	1.191	0.076	31.3	0.771	0.072	8.63	<b>0.502</b>	0.066	6.98	0.542	0.050	<b>6.08</b>	0.533	<b>0.045</b>	6.61
Computing Time	Low			Low			Medium			High			Highest		

a. Sample size: N = 768, Prediction Horizon of 90 s.